

# Drivers of Surface Ocean Mercury Concentrations and Air–Sea Exchange in the West Atlantic Ocean

Anne L. Soerensen,<sup>\*,†,‡</sup> Robert P. Mason,<sup>§</sup> Prentiss H. Balcom,<sup>§</sup> and Elsie M. Sunderland<sup>†,‡</sup>

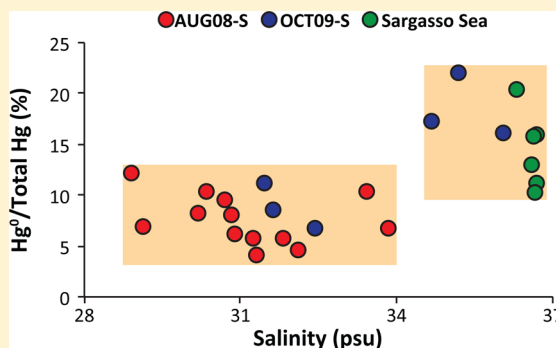
<sup>†</sup>Department of Environmental Health, Harvard School of Public Health, Boston, Massachusetts 02215, United States

<sup>‡</sup>School of Engineering and Applied Sciences, Harvard University, Cambridge, Massachusetts 02138, United States

<sup>§</sup>Department of Marine Sciences, University of Connecticut, 1080 Shennecossett Road, Groton, Connecticut 06340, United States

## S Supporting Information

**ABSTRACT:** Accurately characterizing net evasion of elemental mercury ( $\text{Hg}^0$ ) from marine systems is essential for understanding the global biogeochemical mercury (Hg) cycle and the pool of divalent Hg ( $\text{Hg}^{\text{II}}$ ) available for methylation. Few high resolution measurements of  $\text{Hg}^0$  are presently available for constraining global and regional flux estimates and for understanding drivers of spatial and temporal variability in evasion. We simultaneously measured high-resolution atmospheric and surface seawater  $\text{Hg}^0$  concentrations as well as the total Hg distribution during six cruises in the West Atlantic Ocean between 2008 and 2010 and examined environmental factors affecting net  $\text{Hg}^0$  formation and evasion. We observed the lowest fraction of Hg as  $\text{Hg}^0$  ( $7.8 \pm 2.4\%$ ) in the near-coastal and shelf areas that are influenced by riverine inputs. Significantly higher  $\% \text{Hg}^0$  observed in open ocean areas ( $15.8 \pm 3.9\%$ ) may reflect lower dissolved organic carbon (DOC) in offshore environments, which is known to affect both the reducible  $\text{Hg}^{\text{II}}$  pool and redox kinetics. Calculated  $\text{Hg}^0$  evasion changed by more than a factor of 3 between cruises (range:  $2.1 \pm 0.7$  to  $6.8 \pm 5.1 \text{ ng m}^{-2} \text{ h}^{-1}$ ), driven mainly by variability in  $\text{Hg}^0$  and wind speed. Our results suggest that further mechanistic understanding of the role of DOC on Hg redox kinetics in different types of marine environments is needed to explain variability in  $\text{Hg}^0$  concentrations and improve global estimates of air–sea exchange.



## INTRODUCTION

Oceanic evasion of gaseous elemental Hg ( $\text{Hg}^0$ ) accounts for  $\sim 1/3$  of annual global atmospheric Hg emissions and reduces the amount of  $\text{Hg}^{\text{II}}$  available for conversion to methylmercury, a neurotoxin that bioaccumulates in marine fish.<sup>1</sup> Air–sea exchange of  $\text{Hg}^0$  extends the lifetime of Hg in actively cycling surface reservoirs and enhances the global distribution of anthropogenic sources.<sup>2</sup> Few high resolution measurements of  $\text{Hg}^0$  are presently available for constraining global and regional flux estimates and for understanding drivers of spatial and temporal variability in evasion.<sup>3,4</sup> Here we use data from six cruises in two contrasting regions of the western Atlantic Ocean to examine variability in  $\text{Hg}^0$  concentrations and air–sea exchange in coastal, shelf, and open ocean waters.

Few prior studies of the distribution of  $\text{Hg}^0$  in coastal and open ocean waters have visited the same location more than once.<sup>5,6</sup> Different water masses in open ocean regions exhibit substantial variability in subsurface Hg concentrations<sup>4,7,8</sup> as do surface waters due to seasonal mixing with subsurface waters, inputs from atmospheric deposition, and losses from  $\text{Hg}^0$  evasion.<sup>9–11</sup> Longer term variations in seawater Hg concentrations reflect the impact of changes in anthropogenic inputs and also affect the extent of  $\text{Hg}^0$  evasion at the surface.<sup>12</sup> Higher surface ocean productivity increases Hg removal through

particle scavenging and may also enhance biological  $\text{Hg}^0$  reduction.<sup>13</sup>

In coastal environments, temporal differences in Hg concentrations are more pronounced than in the open-ocean both seasonally due to variability in freshwater inputs and changes in anthropogenic inputs at ocean margins over longer time scales.<sup>14–16</sup> Elevated total Hg concentrations in coastal regions reflect inputs from rivers, submerged groundwater discharge, and point sources such as wastewater and industrial effluents.

Net  $\text{Hg}^0$  concentrations in seawater reflect the influence of environmental factors such as wind speed, temperature, photochemistry, productivity, microbial activity on redox chemistry, and the rate of gas transfer at the air–sea interface.<sup>13,17–19</sup> Reduction of  $\text{Hg}^{\text{II}}$  to  $\text{Hg}^0$  is driven by a combination of photolytic and biotic processes, while conversion of  $\text{Hg}^0$  back to  $\text{Hg}^{\text{II}}$  occurs by both photochemical and dark oxidation.<sup>17–22</sup> Both the size of the reducible  $\text{Hg}^{\text{II}}$  pool and the balance of these redox reactions determines the extent of net reduction in seawater.<sup>13,17,23</sup> Prior research shows the

Received: March 28, 2013

Revised: June 6, 2013

Accepted: June 11, 2013

Published: June 11, 2013

reducible  $\text{Hg}^{\text{II}}$  pool is affected by the relative stability of  $\text{Hg}^{\text{II}}$  complexes with both inorganic and organic ligands.<sup>17,24</sup>

The main objective of this study is to better understand spatial and temporal variability in  $\text{Hg}^0$  concentrations and fluxes across coastal, shelf, and open-ocean waters. To do this, we measured short-term and interannual variability in  $\text{Hg}^0$  concentrations and examined associated environmental drivers of changing concentrations and fluxes. Here we present high resolution simultaneous measurements of atmospheric and oceanic  $\text{Hg}^0$ ,  $\text{Hg}$  speciation, wind speed, temperature, salinity, and in situ fluorescence from six cruises in the Gulf of Maine, the New England Shelf, the continental slope region, and the Sargasso Sea between 2008 and 2010.

## METHODS

Figure 1 shows the cruise tracks where we simultaneously measured total gaseous atmospheric  $\text{Hg}$  and dissolved gaseous

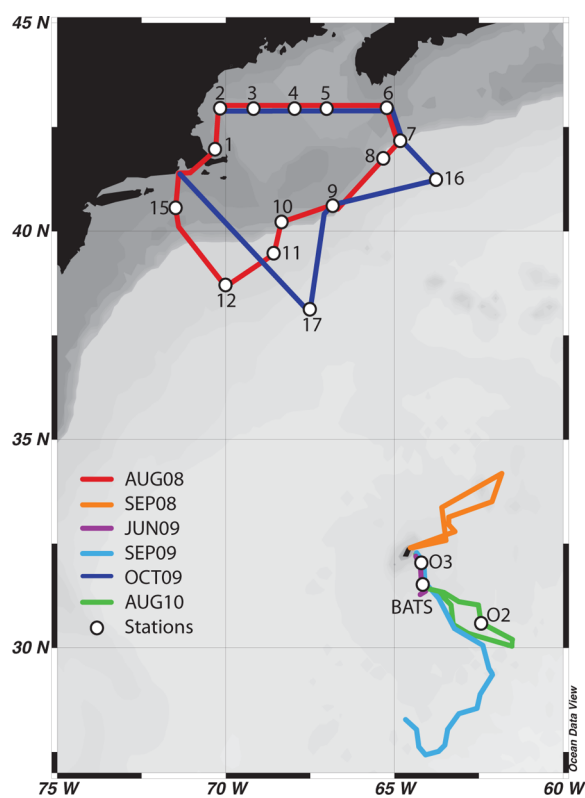


**Figure 1.** Cruise tracks and location of stations during the two shelf cruises (departing from Narragansett, RI) and the four Sargasso Sea cruises (departing from Bermuda). Circles denote sampling stations where we collected surface seawater for total  $\text{Hg}$  analysis.<sup>27</sup> BATS is the station of Bermuda Atlantic Time-Series study.<sup>48</sup> Stations 1–6 and 15 are on the shelf, stations 7–10 are on the shelf slope, and stations 11, 12, 16, and 17 are off the slope.

$\text{Hg}$ , and Table 1 provides details of cruises and sampling dates. We assume dissolved gaseous  $\text{Hg}$  in surface seawater is mainly  $\text{Hg}^0$  because studies have shown that it generally contains <5% dimethylmercury.<sup>17,18,25</sup> On most cruises, the ship was continuously moving except when sampling, which allowed for the collection of data to examine small scale variability in concentrations and speciation. Atmospheric and aqueous  $\text{Hg}^0$  data were collected continuously in the Gulf of Maine, New England shelf, and continental slope regions (denoted AUG08-S and OCT09-S for the August 2008 and October 2009 cruises, respectively) and in the Sargasso Sea (September 2008: SEP08-O; June 2009: JUN09-O; September 2009: SEP09-O; August 2010: AUG10-O). Ancillary data on wind speed, salinity, surface water temperature, and in situ fluorescence (a proxy for *Chla*) were also collected from the ship's surface water intake.

Surface seawater samples for total  $\text{Hg}$  analysis were collected with trace-element clean Go-Flo or Ex-Niskin bottles suspended from a nonmetallic hydrowire, either singly or with a rosette. Samples were processed on board in either a clean van or a sheet-plastic "bubble" supplied with HEPA filtered air. Standard trace-metal-free sampling techniques were followed at all times.<sup>26</sup> Additional details on sampling protocols can be found in Hammerschmidt et al.<sup>27</sup> and Lamborg et al.<sup>28</sup> Water samples for analysis of dissolved  $\text{Hg}$  species (<0.2  $\mu\text{m}$ ) were filtered using acid-washed, plastic vacuum filtration units (GE polycarbonate (PCTE) membranes (0.2  $\mu\text{m}$ )), transferred to glass storage bottles, preserved with 0.5% HCl (trace metal grade), and refrigerated. Unfiltered samples were transferred directly from 2 L Teflon (FEP) holding bottles to glass storage bottles and preserved in the same way. We analyzed total  $\text{Hg}$  using 100–200 mL aliquots of filtered or unfiltered water digested chemically with 0.2 mL of bromine monochloride ( $\text{BrCl}$ ) per 100 mL of sample, and subsequently excess oxidant was neutralized with 0.1 mL of hydroxylamine hydrochloride ( $\text{NH}_2\text{OH}\cdot\text{HCl}$ ) per 100 mL of sample (12% weight/volume solution). Sample  $\text{Hg}$  was reduced to  $\text{Hg}^0$  with stannous chloride ( $\text{SnCl}_2$ ) and quantified by cold vapor atomic fluorescence spectrometry (CVAFS) using a TEKTRAN 2500. Based on two separate assessments, the average method detection limit is 0.15 pM, and the average reagent blank (includes  $\text{BrCl}$ ,  $\text{NH}_2\text{OH}\cdot\text{HCl}$ , and trace metal HCl at 0.5%) is 0.35 pM. We regularly participate in international intercalibration exercises (e.g.,<sup>28</sup>) for all  $\text{Hg}$  species which have validated our analytical methods.

We measured atmospheric  $\text{Hg}^0$  with 5 min resolution using a Tekran 2537A mercury vapor analyzer. The instrument was calibrated daily using the internal calibration source and had a detection limit of <0.2  $\text{ng m}^{-3}$ . For aqueous  $\text{Hg}^0$ , we collected seawater from the ship's intake at 5 m depth and used the automatic continuous equilibrium system with a 5-min temporal resolution described in detail in Andersson et al.<sup>29,30</sup> Instrument calibration and detection limit were as described for atmospheric measurements. We aggregated all high-resolution measurements including underway measure-

**Table 1.** Summary of Sampling Dates and Vessels for Six West Atlantic Cruises

	AUG08-S	SEP08-O	JUN09-O	SEP09-O	OCT09-S	AUG10-O
location	shelf	open ocean	open ocean	open ocean	shelf	open ocean
dates	Aug 17–27	Sept 21–26	June 24–27	Aug 31–Sept 4	Sept 29–Oct 7	Aug 4–9
year	2008	2008	2009	2009	2009	2010
ship	R/V Endeavor	R/V Atlantic Explorer	R/V Atlantic Explorer	R/V Atlantic Explorer	R/V Endeavor	R/V Atlantic Explorer

ments of salinity, temperature, and in situ fluorescence into 1-h averages for statistical analyses. Averaging over 1 h is reasonable, as the short-term variability in the measurements was small (<3% variability typically for 1 h,  $n = 12$ ). Additionally, this analytical variability is much less than that found during individual cruises, indicating that the changes observed over longer time scales are not due to analytical factors. Comparison of continuous and manual batch measurements also showed that the underway measurements are consistent with the batch data ( $r^2 = 0.85$ ,  $p < 0.001$ ,  $n = 15$ ), as found by others.<sup>30</sup>

Air–sea fluxes were calculated using the Nightingale et al.<sup>31</sup> parametrization for instantaneous wind speeds, Henry's law coefficient for  $\text{Hg}^0$ ,<sup>32</sup> a temperature-corrected Schmidt number for  $\text{CO}_2$ ,<sup>33</sup> and the Wilke–Chang method for estimation of a temperature and salinity-corrected  $\text{Hg}^0$  diffusivity.<sup>34</sup> We selected the Nightingale et al.<sup>31</sup> parametrization because it provides a midrange estimate of air–sea exchange.<sup>35,36</sup> Other studies have established that variability in estimated  $\text{Hg}^0$  evasion across gas-exchange models is generally  $\pm 30\%$ ,<sup>16,37,38</sup> which is much less than the ranges of fluxes calculated here ( $\sim 300\%$ ) due to differences in measured  $\text{Hg}^0$ , wind speed, and temperature.

## RESULTS

Figure 2 shows measured spatial distributions of filtered total Hg and dissolved aqueous  $\text{Hg}^0$ . Highest total Hg concentrations were measured on the August 2008 shelf cruise in the Gulf of Maine and on the New England Shelf (Table 2, filtered Hg: 1.3–3.5 pM). Total Hg was significantly lower ( $t$  test for paired means:  $p < 0.0001$ ) during the October 2009 cruise in the same region (Table 2, filtered Hg: 0.45–0.89 pM). Total Hg concentrations measured in the Sargasso Sea were in the same range as the October 2009 shelf cruise (Table 2), with the exception of higher concentrations during the August 2010 sampling period (filtered: 1.2–1.6 pM).

Cruise wide average  $\text{Hg}^0$  concentrations differed significantly ( $t$  test for paired means:  $p < 0.0001$ ) between all cruises (Table 2). Highest  $\text{Hg}^0$  concentrations were observed during the August 2008 shelf cruise ( $160 \pm 60$  fM) and the August 2010 Sargasso Sea cruise ( $196 \pm 34$  fM), and lowest concentrations were measured during the October 2009 shelf cruise ( $90 \pm 24$  fM). Variability in seawater  $\text{Hg}^0$  concentrations was greater on the shelf and slope (40–400 fM) than in the Sargasso Sea (80–260 fM). We did not find any significant difference in  $\text{Hg}^0$  concentrations between night and day (day 06:00–18:00) during any of the cruises.

The fraction of filtered total Hg present as  $\text{Hg}^0$  (% $\text{Hg}^0$ ) was significantly higher ( $t$  test,  $p < 0.0001$ ) in waters with salinities above 34.6 psu ( $15.8 \pm 3.9\%$ ) than at lower salinities ( $7.8 \pm 2.4\%$ ; <33.8 psu) (Figure S1, Supporting Information). Mean % $\text{Hg}^0$  was very similar for the two shelf/slope cruises (OCT09-S = 8.8%  $\text{Hg}^0$  in seawater below 33.8 psu, AUG08-S = 7.6%  $\text{Hg}^0$ ) despite large differences in total Hg concentrations.

Atmospheric  $\text{Hg}^0$  concentrations measured across the four cruises were stable ( $1.4$ – $1.5$  ng  $\text{m}^{-3}$ ) (Table 2). Marine air concentrations were elevated compared to landbased sites at Appledore Island in the Gulf of Maine and Kejimikujik, Nova Scotia ( $\sim 1.1$ – $1.2$  ng  $\text{m}^{-3}$  for the same months as sampling period),<sup>39,40</sup> likely due to oceanic evasion.<sup>12</sup>

Calculated evasion fluxes ranged from 2.1 to 6.8 ng  $\text{m}^{-2} \text{h}^{-1}$  across all cruises (Table 2). As expected, this 3-fold variability is driven mainly by differences in seawater  $\text{Hg}^0$  concentrations

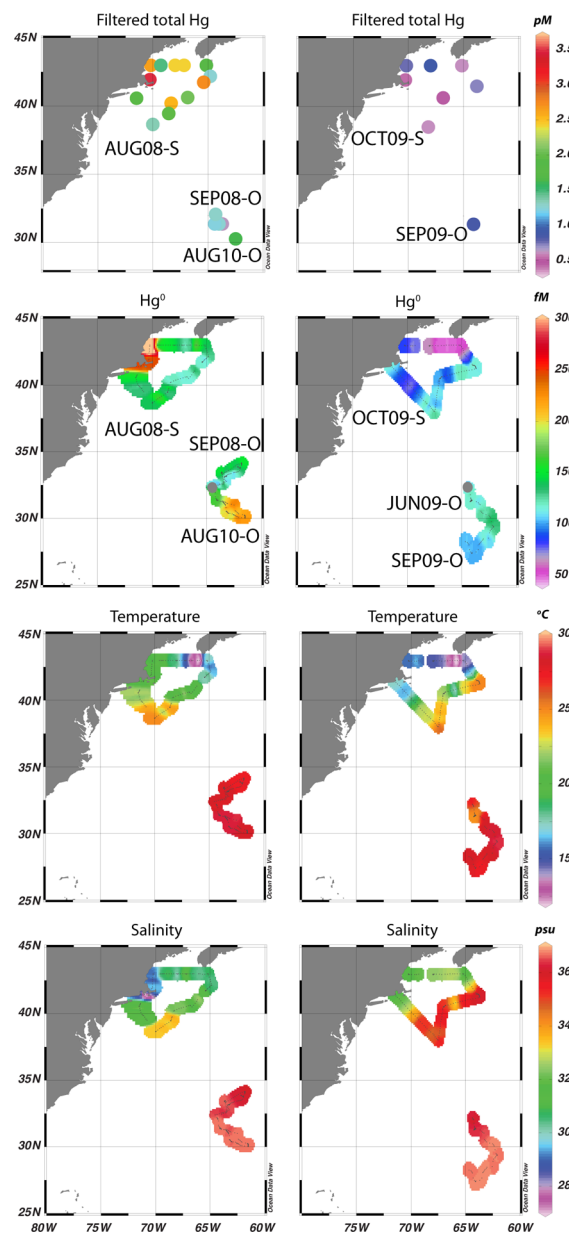


**Figure 2.** Spatial patterns in measured  $\text{Hg}^0$ , filtered total Hg, temperature, and salinity across six cruises in the West Atlantic Ocean.

and wind speeds across the various cruises. The highest overall flux corresponds to the August 2010 sampling period in the Sargasso Sea where elevated seawater  $\text{Hg}^0$  concentrations were observed and wind speeds averaged  $6.2 \pm 2.4$   $\text{m s}^{-1}$  (Table 2). Lowest average evasion fluxes were observed in September 2009 in the Sargasso Sea and October 2009 on the shelf when wind speeds and seawater  $\text{Hg}^0$ , respectively, were lowest among all the cruises.

## DISCUSSION

### Variability in Coastal and Shelf Hg Concentrations.

The observed  $\sim 3$ -fold difference in total Hg and  $\text{Hg}^0$  concentration between the two shelf cruises reflects interannual variability in freshwater inputs. Salinity was lower (e.g., 2.6 psu at Station 2) in August 2008 compared to October 2009 at overlapping sampling stations due to anomalously high rainfall in July of 2008 and correspondingly elevated freshwater

**Table 2. Summary of Observed Mercury and Environmental Data for Six West Atlantic Ocean Cruises (numerical average  $\pm$  stdv)<sup>a</sup>**

	AUG08-S	SEP08-O	JUN09-O	SEP09-O	OCT09-S	AUG10-O
Hg <sup>0</sup> air (ng m <sup>-3</sup> )	1.4 $\pm$ 0.2 <sup>b</sup>	1.5 $\pm$ 0.1	1.4 $\pm$ 0.1	NA <sup>c</sup>	1.4 $\pm$ 0.2 <sup>b</sup>	NA <sup>c</sup>
unfiltered total Hg (pM)	1.8–4.7	NA	NA	NA	0.58–2.32	NA
filtered total Hg (pM)	1.3–3.5	0.63 <sup>d</sup>	NA	0.85	0.45–0.89	1.2–1.6
Hg <sup>0</sup> aq (fM)	160 $\pm$ 60	128 $\pm$ 20	120 $\pm$ 7	111 $\pm$ 14	90 $\pm$ 24	196 $\pm$ 34
flux (ng m <sup>-2</sup> h <sup>-1</sup> )	4.3 $\pm$ 3.4 <sup>b</sup>	3.0 $\pm$ 2.9	4.7 $\pm$ 3.7	2.1 $\pm$ 0.7 <sup>c</sup>	2.2 $\pm$ 1.7 <sup>b</sup>	6.8 $\pm$ 5.1 <sup>c</sup>
saturation (%)	628 $\pm$ 232	617 $\pm$ 122	524 $\pm$ 59	527 $\pm$ 71	368 $\pm$ 129	934 $\pm$ 159
wind speed (m s <sup>-1</sup> )	6.3 $\pm$ 3.2	5.1 $\pm$ 2.3	7.4 $\pm$ 3.3	5.2 $\pm$ 0.9	6.6 $\pm$ 2.3	6.2 $\pm$ 2.4
temperature (°C)	20.2 $\pm$ 3.1	27.7 $\pm$ 0.3	24.4 $\pm$ 0.2	28.1 $\pm$ 0.5	19.6 $\pm$ 4.3	28.3 $\pm$ 0.4
salinity (psu)	31.1 $\pm$ 2.7	36.3 $\pm$ 0.2	36.2 $\pm$ 0.3	36.6 $\pm$ 0.2	33.9 $\pm$ 1.7	36.7 $\pm$ 0.1
Chla <sup>e</sup> (mg m <sup>-3</sup> )	0.16–3.97	<0.08	<0.08	<0.08	0.28–7.43	<0.08

<sup>a</sup>NA = not available. <sup>b</sup>Atmospheric Hg<sup>0</sup> was only measured during less than half of the cruise, and air–sea flux calculation was based on averages for the cruise. <sup>c</sup>Atmospheric Hg<sup>0</sup> concentrations for air–sea flux calculations were estimated based on Hg<sup>0</sup> concentrations from the other cruises in the same region. This is reasonable because atmospheric concentrations varied by only 3–5% across cruises, leading to <2% difference in evasion fluxes. <sup>d</sup>Total Hg from 7 m depth during the September 2008 cruise at BATS station (Lamborg Pers. Comm.). <sup>e</sup>Chla is taken from 4 km resolution Modis-Aqua data.<sup>46</sup>

**Table 3. Summary of Total Hg, Hg<sup>0</sup>, and Air–Sea Exchange Estimates for Coastal, Shelf, and Open Ocean Stations in the Atlantic Ocean<sup>a</sup>**

place	time	unfiltered total Hg (pM)	filtered total Hg (pM)	Hg <sup>0</sup> (fM)	evasion (ng m <sup>-2</sup> h <sup>-1</sup> )	reference
<i>Open Ocean</i>						
East Atlantic	Nov 2005	~1.50				Pohl et al. <sup>62</sup>
East Atlantic (0–50°N)	Nov 2008	~1.50		80 $\pm$ 20	~1.9 <sup>b</sup>	Kuss et al. <sup>5</sup>
East Atlantic (0–50°N)	May 2009	~0.80		20 $\pm$ 5	~0.1 <sup>b</sup>	Kuss et al. <sup>5</sup>
East Atlantic (60–63°N)	July 2005			58 $\pm$ 10	0.42 $\pm$ 0.36 <sup>b</sup>	Andersson et al. <sup>59</sup>
West Atlantic (BATS)	June 2008		0.81			Lamborg et al. <sup>28</sup>
West Atlantic (BATS)	1999–2000		0.95–1.45	244 $\pm$ 99	1.67–5.57 <sup>c</sup>	Mason et al. <sup>19</sup>
<i>Coast and Shelf</i>						
Coastal France	Feb 2000		1.35 $\pm$ 0.35	<DL–500		Laurier et al. <sup>63</sup>
Coastal France	Aug 2000		1.59 $\pm$ 0.33			Laurier et al. <sup>63</sup>
North Sea and English Channel	Apr 1998	2.27 $\pm$ 0.51	1.59 $\pm$ 0.17			Leermakers et al. <sup>14</sup>
North Sea and English Channel	Sept 1998	1.92 $\pm$ 0.81	1.30 $\pm$ 0.30			Leermakers et al. <sup>14</sup>
Mid Atlantic Bight shelf	July 1998		~0.50–5.00	~50–1400		Mason et al. <sup>19</sup>
Long Island Sound	Aug 1995			37–550	0.85; 2.86 <sup>d</sup>	Rolfhus and Fitzgerald <sup>37</sup>

<sup>a</sup>DL = detection limit. <sup>b</sup>Average fluxes calculated using the Nighthingale et al.<sup>31</sup> model. <sup>c</sup>Based on monthly averaged reported fluxes calculated using the Wanninkhof et al.<sup>35</sup> model. <sup>d</sup>Based on annually averaged reported flux calculated using the Liss and Merlivat<sup>36</sup> and Wanninkhof et al.<sup>35</sup> models, respectively.

discharges.<sup>41,42</sup> Additionally, total suspended solids concentrations (also related to freshwater inputs) were higher in August 2008 (up to 4 mg/L) compared to October 2009 ( $\leq$  1 mg/L).<sup>27</sup> Typically, freshwater inputs to the Gulf of Maine peak in April and May and are lowest in July–October.<sup>42</sup> However, in August 2008 freshwater inflow was equivalent to peak discharges that generally occur in April and May (Figure S2, Supporting Information). These results highlight differences in marine shelf and slope Hg concentrations attributable to seasonal and interannual variability in freshwater discharges.

Declining total Hg with increasing salinity measured across all stations ( $R^2 = 0.36$ ,  $P < 0.005$ ,  $n = 25$ ) reflects decreasing inputs from rivers moving from the coast into the open ocean. Total Hg concentrations measured by others in Gulf of Maine tributaries are substantially higher than we observed in marine waters (unfiltered range: 7.8–29.1 pM for the outer Bay of

Fundy and up to 93 pM for the contaminated Penobscot river).<sup>16,43</sup> Sunderland et al.<sup>44</sup> estimated that for the entire Gulf of Maine system, on average riverine total Hg accounted for only ~5% of total inputs, with the remaining fractions from inflowing oceanographic inputs, atmospheric deposition, and point sources. By contrast, the freshwater content of seawater analyzed here at station 2 ranged from 20% in August 2008 to 10% October 2009 (Figure 1) and accounted for difference of 1.9 pM in total Hg, suggesting a relative contribution of >70% from rivers at this location in August 2008. Harris et al.<sup>45</sup> reported similar findings for the Gulf of Mexico where on a system-wide annual basis, total Hg inputs from rivers were a relatively minor contributor but over smaller spatial scales were the dominant contributor to inputs.

Despite relatively greater Hg inputs at coastal margins, total Hg concentrations measured during the October 2009 shelf



Table 4. Results of Multiple and Linear Regression Analysis (all significant results at the  $p < 0.05$  level are shown)<sup>a</sup>

data set	linear regression analysis					multiple regression analysis		
	temperature (R)	salinity (R)	wind speed (R)	fluorescence (R)	Hg <sup>0</sup> (R)	best model fit	(R)	<i>n</i>
<i>Continuous Data (Hg<sup>0</sup>)</i>								
all cruises	0.32		0.10	NA	NA	temp – salinity + wind speed	0.68	709
ocean cruises	0.35	0.35	0.26	NA	NA	temp + salinity + wind speed	0.56	359
SEP08-O	–0.53	–0.26	0.64	NA	NA	–temp + wind speed	0.72	107
JUN09-O		–0.40			NA	temp – salinity + wind speed – Chl <sub>a</sub>	0.59	69
SEP09-O	0.64	0.40		–0.44	NA	temp + salinity – Chl <sub>a</sub>	0.78	62
AUG10-O	–0.47		0.42		NA	–temp – salinity + wind speed – Chl <sub>a</sub>	0.79	121
OCT09-S	0.88	0.75		–0.62	NA	NA <sup>b</sup>	NA	155
AUG08-S		–0.65		0.66	NA	temp – salinity + Chl <sub>a</sub>	0.89	195
<i>Filtered Total Hg (station data)</i>								
		–0.60			0.57			26
<i>Unfiltered Total Hg (station data)</i>								
		–0.49			0.67			18

<sup>a</sup>NA = not available. <sup>b</sup>Temperature, salinity, and in situ fluorescence showed multicollinearity (variance inflation factor >4) for the October 2009 shelf cruise.

cruise were similar in magnitude to Sargasso Sea values. This can be explained by the higher relative productivity across the nearshore sites in October 2009 (0.28–7.43 mg m<sup>–3</sup>) and associated particle Hg removal compared to offshore areas (<0.08 mg m<sup>–3</sup>) (Table 2).<sup>46</sup> In August 2008 high total Hg concentrations reflected the combination of lower productivity (0.16–3.97 mg m<sup>3</sup>)<sup>46</sup> and elevated freshwater inputs (~20% freshwater input at Station 2). On a global scale, model results suggest that particle-associated Hg<sup>II</sup> scavenging from the surface ocean is the main vector for transport to subsurface waters, and thus seasonal and interannual variability in productivity is important for characterizing variability in seawater Hg.<sup>13</sup>

**Variability in Offshore Total Hg.** Recent surface water total Hg measurements from the East Atlantic Ocean (Table 3) are comparable to Sargasso Sea measurements from August 2010 reported here, while the total Hg ranges for September (2008, 2009) are similar to the June 2008 Sargasso Sea average (0.81 pM) reported by Lamborg et al.<sup>28</sup> Concentration differences among cruises are not explained by enhanced inputs from atmospheric deposition (precipitation was comparable among cruises<sup>47</sup>) or enhanced mixing with subsurface waters based on observed density profiles from the Bermuda Atlantic Time-Series region where cruises took place.<sup>48</sup>

Total Hg concentrations measured across all cruises are characteristic of the range reported for the Atlantic basin as a whole and reflect variability in concentrations of water masses of different origins sampled over the various field seasons. Variability within cruises can be explained by the crossing of mesoscale vortices (<100 km radius) present within the Sargasso Sea. Further evidence is provided by Acoustic Doppler Current Profiler (ACDP) data. For example, data from September 2009 show several instances of rapid changes in current speed and direction. In one instance, the ship traveled from higher velocity waters (6–7 cm s<sup>–1</sup>, northerly flowing) to low velocity waters (<1 cm s<sup>–1</sup>, easterly to southerly flowing) and then back again to the higher velocity waters over a timespan of 10 h. Water masses sampled therefore differ both between cruises and within individual cruises due to the sampling of different mesoscale features during transit.

**Variability in Percent Hg<sup>0</sup>/Total Hg in Seawater.** Across all cruises, we found a significantly higher proportion of filtered

Hg as Hg<sup>0</sup> (%Hg<sup>0</sup>) in offshore seawater with salinity >34.6 psu (15.8 ± 3.9%) compared to more freshwater influenced areas (7.8 ± 2.4%; <33.8 psu) (Figure S1). These findings imply that Hg<sup>0</sup> evasion will be proportionally higher in open ocean areas with the same Hg<sup>II</sup> concentrations and environmental conditions than those closer to the coast. For example, the lowest Hg<sup>0</sup> across the six cruises is found on the shelf in October 2009 when total Hg concentrations were similar to open ocean cruises (Table 2).

Differences in %Hg<sup>0</sup> noted here are consistent with differences in dissolved organic carbon (DOC) content among coastal, shelf, and offshore water. In general, concentrations in coastal regions (110–150 μM) are higher than those offshore in the Gulf of Maine (55–90 μM) and in the vicinity of Bermuda (60–70 μM).<sup>49,50</sup> While a large fraction of the organic carbon close to the shore is from allochthonous sources, DOC changes around Bermuda are mostly related to changes in primary productivity and seasonal water column mixing rather than freshwater inputs. Decreases in %Hg<sup>0</sup> at lower salinities could be caused by enhanced stability of Hg<sup>II</sup> complexes with certain types of allochthonous DOC in shelf areas, effectively changing the size of the reducible Hg<sup>II</sup> pool.<sup>24,51</sup> In higher salinity waters there appear to be higher concentrations of reactive Hg and reduced abundance of Hg-binding ligands.<sup>24,52</sup> Reduced light penetration and photo-reduction in high DOC waters is also plausible because colored DOC is highly effective at attenuating light penetration in surface waters.<sup>53</sup> Further elucidation of the types and composition of DOC–Hg complexes in coastal and offshore waters is needed to refine our understanding of the effect of DOC on Hg reduction kinetics.

**Controls on Hg<sup>0</sup> Distribution.** Table 4 shows results of linear and multiple regression analysis used to identify the relationships between continuously measured Hg<sup>0</sup> concentrations (*n* = 709) and environmental factors (temperature, salinity, wind speed, and in situ fluorescence). Because fluorescence was not calibrated against measurements of Chl<sub>a</sub>, it is a relative value and could only be included in the analysis of Hg<sup>0</sup> variability for individual cruises. Here we use fluorescence as a proxy for phytoplankton biomass,<sup>54</sup> which in turn affects particle-associated scavenging of Hg<sup>II</sup> from surface waters and biological production of Hg<sup>0</sup>.

Temperature and salinity are significant predictors of variability in  $\text{Hg}^0$  concentrations across all cruises and for individual cruises (Table 4), but the association with  $\text{Hg}^0$  variability is both positive and negative across individual cruises. Temperature and salinity are positively associated with  $\text{Hg}^0$  concentrations when all Sargasso Sea cruises are combined but do not explain the majority of the variability in  $\text{Hg}^0$  concentrations ( $R = 0.56$ ).

Mechanistically, higher seawater temperatures are expected to increase net reduction as well as enhance the diffusivity of  $\text{Hg}^0$ , increasing increasing production from  $\text{Hg}^{\text{II}}$  and evasion. Changes in salinity can also affect Hg complexation with different ligands. Observed correlations are unlikely to reflect these mechanistic relationships given their mixed directions. Maximum temperature differences across the Sargasso Sea cruises were  $<4\text{ }^\circ\text{C}$  (Table 2), which we calculated would lead to  $<15\%$  change in evasion rates. Similarly, salinity differences across the Sargasso Sea cruises are  $\sim 0.5$  psu and unlikely to result in major differences in the dominant  $\text{Hg}^{\text{II}}$  complexes in seawater and associated reduction kinetics.<sup>55</sup> Neither variable therefore accounts for the observed variability in  $\text{Hg}^0$  concentrations across all Sargasso Sea cruises.

Instead, given that temperature and salinity are also effective tracers of the differences in water masses sampled over the cruises, we conclude that the statistical relationships likely reflect different water masses sampled with variable  $\text{Hg}^{\text{II}}$  available for reduction. This is further supported by the well-known occurrence of both cyclonic and anticyclonic vortices in the vicinity of Bermuda<sup>56</sup> that are encountered and crossed during cruises, as indicated by ACDP data described above.

For the August 2008 shelf/slope cruise, when total Hg concentrations were elevated, there is no significant relationship with temperature in the linear regression analysis (Table 4). Variability in  $\text{Hg}^0$  concentrations for this cruise are likely driven by  $\text{Hg}^{\text{II}}$  inputs from freshwater discharges (similar to total Hg) indicated by the negative association with salinity.

Wind speed both enhances the efficiency of air–sea  $\text{Hg}^0$  exchange by creating turbulence in surface waters (negative association with  $\text{Hg}^0$ ) and facilitates mixing with deeper water that can provide additional  $\text{Hg}^{\text{II}}$  substrate for reduction when near surface waters are depleted (positive association with  $\text{Hg}^0$ ). We found a significant positive association between wind speed and  $\text{Hg}^0$  in multiple regression models for all cruises, for all Sargasso Sea cruises together, and when Sargasso Sea cruises are analyzed individually (with the exception of the September 2009 cruise where wind speed was not significant) (Table 4). These findings suggest that, across the sites studied, elevated winds are predominantly driving enhanced  $\text{Hg}^0$  and  $\text{Hg}^{\text{II}}$  supply through mixing with deeper waters within the mixed layer rather than enhanced  $\text{Hg}^0$  loss through evasion (Table 4). This phenomenon is supported by high-resolution measurements of CO in the surface mixed layer near Bermuda that show variability in concentrations within the mixed layer.<sup>57</sup> Wind speed is not a significant predictor in the multiple regression analyses of  $\text{Hg}^0$  concentrations for the shelf cruises, likely because freshwater inputs were more important for  $\text{Hg}^{\text{II}}$  supply than wind-driven mixing. High-resolution profiles of surface ocean  $\text{Hg}^0$  concentrations, in concert with measurement of unreactive gases, would further confirm the variable effects of wind on air–sea exchange and surface water mixing.

Fluorescence is negatively associated with  $\text{Hg}^0$  concentrations for individual Sargasso Sea cruises in the multiple regression analysis except for September 2008 when it is not

significant. Although biotic reduction is known to occur in seawater,<sup>17,58</sup> photochemical processes are much more rapid and tend to dominate overall reduction except under conditions of low light penetration and extremely high productivity.<sup>13</sup> Increased productivity decreases light penetration in the surface ocean,<sup>53</sup> diminishing photoreduction and associated  $\text{Hg}^0$  formation, and also decreases the pool available for reduction through the formation of stable  $\text{Hg}^{\text{II}}$ –DOC complexes. Such processes likely account for the negative association between in situ fluorescence and  $\text{Hg}^0$  variability reported for the open ocean cruises.

For the August 2008 shelf cruise, the positive association between  $\text{Hg}^0$  variability and in situ fluorescence likely indirectly reflects the high  $\text{Hg}^{\text{II}}$ , nutrient and DOC signal from rivers that mixes with lower  $\text{Hg}^{\text{II}}$ , nutrient and DOC from the Gulf rather than a causal association in the water column (Figure S3, Supporting Information). Accordingly, we see the expected negative correlation between fluorescence and  $\text{Hg}^0$  variability in the linear regression during the October 2009 shelf cruise when total Hg inputs from rivers are diminished (Table 4).

#### Challenges for Estimating Annual Evasion Fluxes.

Evasion rates calculated here (Table 2) fall within the range of estimates from the past decade (Table 3) but are higher than those found during recent cruises in the East Atlantic.<sup>5,59</sup> Accurately characterizing net evasion of  $\text{Hg}^0$  from marine systems on an annual basis is essential for understanding the time scales of anthropogenic Hg cycling through biologically relevant surface compartments<sup>2</sup> and the pool of  $\text{Hg}^{\text{II}}$  available for methylation.<sup>10</sup> This requires extrapolating limited observational snapshots of  $\text{Hg}^0$  concentration and short-term flux measurements to larger spatial and temporal scales.

Previous studies have shown that variability in gas exchange model parametrization leads to a systematic difference in  $\text{Hg}^0$  evasion of  $\sim 30\%$ .<sup>16,37,38</sup> To develop a complementary understanding of how daily variability in temperature, wind speed, seawater, and atmospheric  $\text{Hg}^0$  affect calculated evasion rates, we examined the daily standard deviation of 5-min resolution measurements collected here. We use the air–sea exchange model parametrization described in the Methods and do not compare differences across models, where uncertainty has already been characterized. On a daily basis, the impact of stochasticity in atmospheric and aquatic  $\text{Hg}^0$  and seawater temperature on estimated evasion are all less than the 30% difference in flux due to the choice of gas exchange model. The use of instantaneous (5-min resolution) wind speeds changes estimated daily  $\text{Hg}^0$  flux by 39–72%. In general, these results suggest that daily averaging of information on temperature and atmospheric and aqueous  $\text{Hg}^0$  concentrations is sufficient to estimate air–sea exchange within the bounds of our current mechanistic understanding of physical exchange processes.

Average evasion flux estimates across the six cruises vary by more than a factor of 3 (Table 2). This variability is primarily a function of differences in wind speed and seawater  $\text{Hg}^0$  and to a lesser extent temperature. Using cruise-wide averages for temperature, wind speed, and aqueous  $\text{Hg}^0$  results in a 4–22% difference in modeled evasion compared to fluxes estimated based on 1-h data for these model inputs (Table 2). These results again suggest that coarser resolution data provide reasonable estimates of fluxes across sampling periods. However, seasonal and interannual variability in evasion is large and greatly exceeds the variability introduced by short-term stochasticity in environmental parameters and  $\text{Hg}^0$  concentrations and uncertainty in gas exchange model parametrization.

Additional field data supporting enhancement of mechanistic models<sup>13</sup> that simulate factors controlling seasonal and interannual variability in aqueous Hg<sup>0</sup> redox kinetics are thus essential for refining estimates of global air–sea exchange.

Our results indicate that high Hg<sup>0</sup> concentrations (leading to high evasion) in near-coastal regions of the August 2008 shelf cruise are due to elevated total Hg inputs from rivers. This is similar to findings from other studies that have proposed shelf areas and closed seas have elevated aerial evasion fluxes compared to the open ocean.<sup>6,29</sup> However, the impact of spatially variable differences in seawater chemistry on Hg<sup>0</sup> diffusivity and gas transfer velocity needs to be better accounted for in Hg<sup>0</sup> evasion flux estimates. For example, Frew<sup>60</sup> showed that the gas transfer velocity on the shelf and close to the New England coast decreased to ~70% and ~20%, respectively, of that in the open ocean due to differences in DOC content and surface film dynamics,<sup>60</sup> which vary with seasonal dependent riverine inputs.<sup>61</sup> Correcting for potential changes in gas transfer velocity using DOC concentrations for the August 2008 shelf cruise (using a linear relationship between salinity and DOC reported for the Gulf of Maine by Dai and Nelson<sup>49</sup>) leads to 35–40% decrease in the evasion flux shown in Table 2. Overall, better understanding of how differences in the composition of DOC and organic acids in marine waters effects the reducible pool of Hg<sup>II</sup> and resulting evasion fluxes is needed.

## ■ ASSOCIATED CONTENT

### ● Supporting Information

Additional information, including underway measurements and station surface measurements. This material is available free of charge via the Internet at <http://pubs.acs.org>.

## ■ AUTHOR INFORMATION

### Corresponding Author

\*E-mail: [alsoeren@hsph.harvard.edu](mailto:alsoeren@hsph.harvard.edu).

### Notes

The authors declare no competing financial interest.

## ■ ACKNOWLEDGMENTS

We acknowledge financial support from the U.S. National Science Foundation, Chemical Oceanography division (NSF grants no. 0728750 and 1130549). We thank Maria Andersson, Genevieve Bernier, Susan Gichuki, Michael Finiguerra, Kathleen Gosnell, and Allan Hutchins (UCONN); Tristan Kading, Kathleen Munson, and Carl Lamborg (WHOI); Melissa Tabatchnick and Katlin Bowman (Wright State Univ.); Lynn Butler (Univ. of Rhode Island, GSO); captains, science technicians, and crews of the *R/V Endeavor* and *R/V Atlantic Explorer*; William Fitzgerald (UCONN) and Chad Hammerschmidt (Wright State Univ.) for allowing us to participate in their cruises aboard *R/V Endeavor* (NSF grant no. 0752116) and for using total Hg data from these cruises. We thank Helen Amos for helpful discussions.

## ■ REFERENCES

(1) Mahaffey, K. R.; Sunderland, E. M.; Chan, H. M.; Choi, A. L.; Grandjean, P.; Marien, K.; Oken, E.; Sakamoto, M.; Schoeny, R.; Weihe, P.; Yan, C. H.; Yasutake, A. Balancing the Benefits of N-3 Polyunsaturated Fatty Acids and the Risks of Methylmercury Exposure from Fish Consumption. *Nutr. Rev.* **2011**, *69* (9), 493–508.

(2) Amos, H. M.; Jacob, D. J.; Streets, D. G.; Sunderland, E. M. Legacy Impacts of All-Time Anthropogenic Emissions on the Global Mercury Cycle. *Biogeochem. Cycles* **2013**, *27*, 1–12.

(3) Qureshi, A.; MacLeod, M.; Sunderland, E. M.; Konrad, H. Exchange of Elemental Mercury between the Oceans and the Atmosphere. In *Environmental Chemistry and Toxicology of Mercury*; Liu, G.; Cai, Y.; O'Driscoll, N. J., Eds.; John Wiley & Sons, Inc: Hoboken, NJ, 2011; pp 389–421.

(4) Mason, R. P.; Fitzgerald, W. F. The Distribution and Biogeochemical Cycling of Mercury in the Equatorial Pacific-Ocean. *Deep Sea Res., Part I* **1993**, *40* (9), 1897–1924.

(5) Kuss, J.; Zulficke, C.; Pohl, C.; Schneider, B. Atlantic Mercury Emission Determined from Continuous Analysis of the Elemental Mercury Sea-Air Concentration Difference within Transects between 50 Degrees N and 50 Degrees S. *Glob. Biogeochem. Cycles* **2011**, DOI: 10.1029/2010GB003998.

(6) Tseng, C. M.; Lamborg, C. H.; Hsu, S. C. A Unique Seasonal Pattern in Dissolved Elemental Mercury in the South China Sea, a Tropical and Monsoon-Dominated Marginal Sea. *Geophys. Res. Lett.* **2013**, *40*, 167–172.

(7) Cossa, D.; Heimbürger, L. E.; Lannuzel, D.; Rintoul, S. R.; Butler, E. C. V.; Bowie, A. R.; Averty, B.; Watson, R. J.; Remenyi, T. Mercury in the Southern Ocean. *Geochim. Cosmochim. Acta* **2011**, *75* (14), 4037–4052.

(8) Sunderland, E. M.; Krabbenhoft, D. P.; Moreau, J. W.; Strode, S. A.; Landing, W. M. Mercury Sources, Distribution, and Bioavailability in the North Pacific Ocean: Insights from Data and Models. *Glob. Biogeochem. Cycles* **2009**, *23*, artn Gb2010; doi: 10.1029/2008gb003425.

(9) Sunderland, E. M.; Mason, R. P. Human Impacts on Open Ocean Mercury Concentrations. *Glob. Biogeochem. Cycles* **2007**, *21* (4), artn Gb4022; doi: 10.1029/2006gb002876.

(10) Mason, R. P.; Choi, A. L.; Fitzgerald, W. F.; Hammerschmidt, C. R.; Lamborg, C. H.; Soerensen, A. L.; Sunderland, E. M. Mercury Biogeochemical Cycling in the Ocean and Policy Implications. *Environ. Res. Lett.* **2012**, *119*, 101–17.

(11) Laurier, F. J. G.; Mason, R. P.; Gill, G. A.; Whalin, L. Mercury Distributions in the North Pacific Ocean - 20 Years of Observations. *Mar. Chem.* **2004**, *90* (1–4), 3–19.

(12) Soerensen, A. L.; Jacob, D. J.; Streets, D. G.; Witt, M. L. I.; Ebinghaus, R.; Mason, R. P.; Andersson, M.; Sunderland, E. M. Multi-Decadal Decline of Mercury in the North Atlantic Atmosphere Explained by Changing Subsurface Seawater Concentrations. *Geophys. Res. Lett.* **2012**, *39*; doi: 10.1029/2012GL053736.

(13) Soerensen, A. L.; Sunderland, E. M.; Holmes, C. D.; Jacob, D. J.; Yantosca, R. M.; Skov, H.; Christensen, J. H.; Strode, S. A.; Mason, R. P. An Improved Global Model for Air–Sea Exchange of Mercury: High Concentrations over the North Atlantic. *Environ. Sci. Technol.* **2010**, *44* (22), 8574–8580.

(14) Leermakers, M.; Galletti, S.; De Galan, S.; Brion, N.; Baeyens, W. Mercury in the Southern North Sea and Scheldt Estuary. *Mar. Chem.* **2001**, *75* (3), 229–248.

(15) Balcom, P. H.; Fitzgerald, W. F.; Vandal, G. M.; Lamborg, C. H.; Rolffus, K. R.; Langer, C. S.; Hammerschmidt, C. R. Mercury Sources and Cycling in the Connecticut River and Long Island Sound. *Mar. Chem.* **2004**, *90* (1–4), 53–74.

(16) Sunderland, E. M.; Dalziel, J.; Heyes, A.; Branfireun, B. A.; Krabbenhoft, D. P.; Gobas, F. A. P. C. Response of a Macrotidal Estuary to Changes in Anthropogenic Mercury Loading between 1850 and 2000. *Environ. Sci. Technol.* **2010**, *44* (5), 1698–1704.

(17) Whalin, L.; Kim, E. H.; Mason, R. Factors Influencing the Oxidation, Reduction, Methylation and Demethylation of Mercury Species in Coastal Waters. *Mar. Chem.* **2007**, *107* (3), 278–294.

(18) Mason, R. P.; Rolffus, K. R.; Fitzgerald, W. F. Methylated and Elemental Mercury Cycling in Surface and Deep-Ocean Waters of the North-Atlantic. *Water, Air, Soil Pollut.* **1995**, *80* (1–4), 665–677.

(19) Mason, R. P.; Lawson, N. M.; Sheu, G. R. Mercury in the Atlantic Ocean: Factors Controlling Air–Sea Exchange of Mercury and



Its Distribution in the Upper Waters. *Deep Sea Res., Part II* **2001**, *48* (13), 2829–2853.

(20) Amyot, M.; Gill, G. A.; Morel, F. M. M. Production and Loss of Dissolved Gaseous Mercury in Coastal Seawater. *Environ. Sci. Technol.* **1997**, *31* (12), 3606–3611.

(21) Amyot, M.; Lean, D. R. S.; Poissant, L.; Doyon, M. R. Distribution and Transformation of Elemental Mercury in the St. Lawrence River and Lake Ontario. *Can. J. Fish. Aquat. Sci.* **2000**, *57*, 155–163.

(22) Lalonde, J. D.; Amyot, M.; Kraepiel, A. M. L.; Morel, F. M. M. Photooxidation of Hg(0) in Artificial and Natural Waters. *Environ. Sci. Technol.* **2001**, *35* (7), 1367–1372.

(23) Qureshi, A.; O'Driscoll, N. J.; MacLeod, M.; Neuhold, Y. M.; Hungerbuhler, K. Photoreactions of Mercury in Surface Ocean Water: Gross Reaction Kinetics and Possible Pathways. *Environ. Sci. Technol.* **2010**, *44* (2), 644–649.

(24) Lamborg, C. H.; Fitzgerald, W. F.; Skoog, A.; Visscher, P. T. The Abundance and Source of Mercury-Binding Organic Ligands in Long Island Sound. *Mar. Chem.* **2004**, *90* (1–4), 151–163.

(25) Mason, R. P.; Sullivan, K. A. The Distribution and Speciation of Mercury in the South and Equatorial Atlantic. *Deep Sea Res., Part II* **1999**, *46* (5), 937–956.

(26) Gill, G. A.; Fitzgerald, W. F. Picomolar Mercury Measurements in Seawater and Other Materials Using Stannous Chloride Reduction and 2-Stage Gold Amalgamation with Gas-Phase Detection. *Mar. Chem.* **1987**, *20* (3), 227–243.

(27) Hammerschmidt, C. R.; Finiguerra, M. B.; Weller, R. L.; Fitzgerald, W. F. Methylmercury Accumulation in Plancton on the Continental Margin of the Northwest Atlantic Ocean. *Environ. Sci. Technol.* **2013**, *47* (8), 3671–3677.

(28) Lamborg, C. H.; Hammerschmidt, C. R.; Gill, G. A.; Mason, R. P.; Gichuki, S. An Intercomparison of Procedures for the Determination of Total Mercury in Seawater and Recommendations Regarding Mercury Speciation During Geotraces Cruises. *Limnol. Oceanogr.: Methods* **2012**, *10*, 90–100.

(29) Andersson, M. E.; Gardfeldt, K.; Wangberg, I.; Sprovieri, F.; Pirrone, N.; Lindqvist, O. Seasonal and Daily Variation of Mercury Evasion at Coastal and Off Shore Sites from the Mediterranean Sea. *Mar. Chem.* **2007**, *104* (3–4), 214–226.

(30) Andersson, M. E.; Gardfeldt, K.; Wangberg, I. A Description of an Automatic Continuous Equilibrium System for the Measurement of Dissolved Gaseous Mercury. *Anal. Bioanal. Chem.* **2008**, *391* (6), 2277–2282.

(31) Nightingale, P. D.; Malin, G.; Law, C. S.; Watson, A. J.; Liss, P. S.; Liddicoat, M. I.; Boutin, J.; Upstill-Goddard, R. C. In Situ Evaluation of Air-Sea Gas Exchange Parameterizations Using Novel Conservative and Volatile Tracers. *Glob. Biogeochem. Cycles* **2000**, *14* (1), 373–387.

(32) Andersson, M. E.; Gardfeldt, K.; Wangberg, I.; Stromberg, D. Determination of Henry's Law Constant for Elemental Mercury. *Chemosphere* **2008**, *73* (4), 587–592.

(33) Poissant, L.; Amyot, M.; Pilote, M.; Lean, D. Mercury Water–Air Exchange over the Upper St. Lawrence River and Lake Ontario. *Environ. Sci. Technol.* **2000**, *34* (15), 3069–3078.

(34) Wilke, C. R.; Chang, P. Correlation of Diffusion Coefficients in Dilute Solutions. *AIChE J.* **1955**, *1* (2), 264–270.

(35) Wanninkhof, R. Relationship between Wind-Speed and Gas-Exchange over the Ocean. *J. Geophys. Res. Oceans* **1992**, *97* (C5), 7373–7382.

(36) Liss, P. S.; Merlivat, L. Air-Sea Exchange Rates: Introduction and Synthesis. In *The Role of Air-Sea Exchange in Geochemical Cycling*; Buat-Menard, P., Ed.; Reidel Publishing Company: Dordrecht, 1986; pp 113–127.

(37) Rolffhus, K. R.; Fitzgerald, W. F. The Evasion and Spatial/Temporal Distribution of Mercury Species in Long Island Sound, Ct-Ny. *Geochim. Cosmochim. Acta* **2001**, *65* (3), 407–418.

(38) Strode, S. A.; Jaegle, L.; Selin, N. E.; Jacob, D. J.; Park, R. J.; Yantosca, R. M.; Mason, R. P.; Slemr, F. Air-Sea Exchange in the

Global Mercury Cycle. *Glob. Biogeochem. Cycles* **2007**, *21* (1); doi: 10.1029/2006GB002766.

(39) Mao, H.; Talbot, R. Speciated Mercury at Marine, Coastal, and Inland Sites in New England - Part 1: Temporal Variability. *Atmos. Chem. Phys.* **2012**, *12* (11), 5099–5112.

(40) Cole, A. S.; Steffen, A.; Pfaffhuber, K. A.; Berg, T.; Pilote, M.; Poissant, L.; Tordon, R.; Hung, H. Ten-Year Trends of Atmospheric Mercury in the High Arctic Compared to Canadian Sub-Arctic and Mid-Latitude Sites. *Atmos. Chem. Phys.* **2013**, *13*; doi: 10.5194/acp-13-1535-2013.

(41) NOAA: National Weather Service, Advance Hydrologic Prediction Service Website; <http://water.weather.gov/precip/> (access date: December 2012).

(42) USGS: Water Data for USA, National Water Information System Website; <http://nwis.waterdata.usgs.gov/nwis> (access date: December 2012).

(43) Bodaly, R. A.; Rudd, J. W. M.; Fisher, N. S.; Whipple, C. G. *Penobscot River Mercury Study. Phase 1 of the Study: 2006–2007*, 2008.

(44) Sunderland, E. M.; Amirbahman, A.; Burgess, N. M.; Dalziel, J.; Harding, G.; Jones, S. H.; Kamai, E.; Karagas, M. R.; Shi, X.; Chen, C. Y. Mercury Sources and Fate in the Gulf of Maine. *Environ. Res.* **2012**, *119*, 27–41.

(45) Harris, R.; Pollman, C.; Hutchinson, D.; Landing, W.; Axelrad, D.; Morey, S. L.; Dukhovskoy, D.; Vijayaraghavan, K. A Screening Model Analysis of Mercury Sources, Fate and Bioaccumulation in the Gulf of Mexico. *Environ. Res.* **2012**, *119*, 53–63.

(46) Acker, J. G.; Leptoukh, G. Online Analysis Enhances Use of Nasa Earth Science Data. *EOS, Trans. Am. Geophys. Union* **2007**, *88* (2), 14–17.

(47) Bermuda Weather Service: Climate Data Website; <http://www.weather.bm/climate.asp> (access date: March 2013).

(48) Bermuda Institute of Oceanic Science, Bermuda Atlantic Time-Series Study Website; <http://bats.bios.edu/index.html> (access date: October 2011).

(49) Dai, M. H.; Benitez-Nelson, C. R. Colloidal Organic Carbon and Th-234 in the Gulf of Maine. *Mar. Chem.* **2001**, *74* (2–3), 181–196.

(50) Goldberg, S. J.; Carlson, C. A.; Hansell, D. A.; Nelson, N. B.; Siegel, D. A. Temporal Dynamics of Dissolved Combined Neutral Sugars and the Quality of Dissolved Organic Matter in the Northwestern Sargasso Sea. *Deep Sea Res., Part I* **2009**, *56* (5), 672–685.

(51) Ravichandran, M. Interactions between Mercury and Dissolved Organic Matter - a Review. *Chemosphere* **2004**, *55* (3), 319–331.

(52) Balcom, P. H.; Hammerschmidt, C. R.; Fitzgerald, W. F.; Lamborg, C. H.; O'Connor, J. S. Seasonal Distributions and Cycling of Mercury and Methylmercury in the Waters of New York/New Jersey Harbor Estuary. *Mar. Chem.* **2008**, *109* (1–2), 1–17.

(53) Branco, A. B.; Kremer, J. N. The Relative Importance of Chlorophyll and Colored Dissolved Organic Matter (C<sub>dom</sub>) to the Prediction of the Diffuse Attenuation Coefficient in Shallow Estuaries. *Estuaries* **2005**, *28* (5), 643–652.

(54) Asher, E. C.; Merzouk, A.; Tortell, P. D. Fine-Scale Spatial and Temporal Variability of Surface Water Dimethylsulfide (DMS) Concentrations and Sea-Air Fluxes in the Ne Subarctic Pacific. *Mar. Chem.* **2011**, *126* (1–4), 63–75.

(55) Fitzgerald, W. F.; Lamborg, C. H.; Hammerschmidt, C. R. Marine Biogeochemical Cycling of Mercury. *Chem. Rev.* **2007**, *107* (2), 641–662.

(56) Luce, D. L.; Rossby, T. On the Size and Distribution of Rings and Coherent Vortices in the Sargasso Sea. *J. Geophys. Res. Oceans* **2008**, DOI: 10.1029/2007JC004171.

(57) Zafriou, O. C.; Xie, H. X.; Nelson, N. B.; Najjar, R. G.; Wang, W. Diel Carbon Monoxide Cycling in the Upper Sargasso Sea near Bermuda at the Onset of Spring and in Midsummer. *Limnol. Oceanogr.* **2008**, *53* (2), 835–850.

(58) Mason, R. P.; Morel, F. M. M.; Hemond, H. F. The Role of Microorganisms in Elemental Mercury Formation in Natural-Waters. *Water, Air, Soil Pollut.* **1995**, *80* (1–4), 775–787.



(59) Andersson, M. E.; Sommar, J.; Gardfeldt, K.; Jutterstrom, S. Air-Sea Exchange of Volatile Mercury in the North Atlantic Ocean. *Mar. Chem.* **2011**, *125* (1–4), 1–7.

(60) Frew, N. M. The Role of Organic Films in Air-Sea Gas Exchange. In *The Sea Surface and Global Change*; Liss, P. S.; Duce, R. A., Eds.; Cambridge University Press: Cambridge, 1997; pp 121–172.

(61) Del Vecchio, R.; Blough, N. V. Spatial and Seasonal Distribution of Chromophoric Dissolved Organic Matter and Dissolved Organic Carbon in the Middle Atlantic Bight. *Mar. Chem.* **2004**, *89* (1–4), 169–187.

(62) Pohl, C.; Croot, P. L.; Hennings, U.; Daberkow, T.; Budeus, G.; v. d. Loeff, M. R. Synoptic Transects on the Distribution of Trace Elements (Hg, Pb, Cd, Cu, Ni, Zn, Co, Mn, Fe, and Al) in Surface Waters of the Northern- and Southern East Atlantic. *J. Mar. Sys.* **2011**, *84* (1–2), 28–41.

(63) Laurier, F. J. G.; Cossa, D.; Gonzalez, J. L.; Breviere, E.; Sarazin, G. Mercury Transformations and Exchanges in a High Turbidity Estuary: The Role of Organic Matter and Amorphous Oxyhydroxides. *Geochim. Cosmochim. Acta* **2003**, *67* (18), 3329–3345.